ISIJ International, Vol. 43 (2003), No. 2, pp. 135–143

Review

Annealing of Cold-worked Austenitic Stainless Steels

Angelo Fernando PADILHA, Ronald Lesley PLAUT and Paulo Rangel RIOS[1)]

Departamento de Engenharia Metalúrgica e de Materiais, Escola Politécnica, Universidade São Paulo, 05508-900, São Paulo, Brazil. E-mail: padilha@usp.br 1) Escola de Engenharia Industrial Metalúrgica de Volta Redonda, Av. dos Trabalhadores, 420, Volta Redonda, RJ, 27255-125 Brazil.

(*Received on August 26, 2002; accepted in final form on October 3, 2002*)

This article reviews the phenomena involved during the annealing of cold worked austenitic stainless steels. Initially the cold worked state is discussed, with special emphasis on the formation of deformation induced martensites. Following, the phenomena of martensite reversion, recovery, recrystallization and grain growth are discussed. The interactions between primary recrystallization and precipitation and between precipitate dissolution and secondary recrystallization are dealt with in detail. Finally, the textures resulting from hot and cold working, and from primary and secondary recrystallization, are presented.

KEY WORDS: austenitic stainless steels; work hardening; recovery; recrystallization; grain growth; texture.

1. Introduction

Austenitic stainless steels (ASSs) usually exhibit excellent corrosion resistance, toughness and weldability. However, the strength level, particularly the yield strength, is relatively low, about 200 MPa, in the annealed state. In order to increase their strength, ASSs are often cold worked after solution annealing. Cold work is a convenient strengthening method since ASSs normally have a high strain-hardening coefficient. After thermomechanical treatment[1–6)] a common steel such as the AISI 304 can have its yield strength increased to about 1 400 MPa, with an elongation over 10%.[1)] During plastic deformation, depending on the steel composition and the cold working variables, some induced martensite can be formed. This martensite is usually called "deformation induced martensite", DIM,[7–24)] and has an important influence on the strain-hardening coefficient and on the formability. ASS sheets are normally supplied in the solution annealed condition but in high temperature service, during heat treatments, during thermomechanical treatments, or even in the heat affected zone (HAZ) of weldments, numerous phases can precipitate.[25–30)] Furthermore, annealing of the work-hardened ASS may lead to the formation of more martensite[31,32)] or even to reversion to austenite of the martensite formed during cooling or after deformation.[33–36)] Depending on the degree of cold working and annealing temperature, there may be also excessive grain growth or even secondary recrystallization.[37,38)]

So, during processing or service, cold worked ASSs may present complex microstructural evolution involving precipitation, recovery, recrystallization and grain growth. The objective of this paper is to examine in detail these phenomena. In addition, the resulting textures associated with hot rolling, cold rolling, recrystallization and grain growth will also be discussed.

2. The Cold Worked State

In many cases, the final heat treatment applied to the ASSs, before usage, is solution annealing. Such a treatment is performed in the temperature range of 1 000 to 1 150°C and, in general, takes less than 1 h. **Figure 1** gives an overall view of the different heat treatments and transformations that occur in the ASSs.

After solution annealing, the ASSs microstructure is constituted of insoluble particles or partially insoluble ones, dispersed in a solid solution that has a low stacking fault energy (SFE) that, in the case of wrought alloys, presents several annealing twins. In the case of stabilized steels (see Table 1), particles are predominantly carbides of the MC type (M=Ti, Nb, V and Zr), nitrides of the MN (M=Ti, Zr) type and carbosulfides of the $M_4C_2S_2$ (M=Ti and Zr) type [30]. Insoluble oxide particles, nearly-round shaped, containing Si, Cr, Ca, Ni or Mn, can be frequently found.[3,25)] These particles have a minor effect on the macroscopic strain-hardening behavior of the ASS, however it changes the dislocation density and distribution around the particles (geometrically necessary dislocations). The main alloying elements, Cr, Ni and Mo, act chiefly through their effect on the SFE, as will be discussed in the following paragraphs.

During cold working of ASSs, stacking faults, stacking-faults bundles or faulted ε-martensite, deformation twins, deformation bands and α' martensite may be formed, besides intensive dislocation multiplication.[1,7–25)]

SFE plays a very important role in the deformation substructure, *i.e.*, in the nature, density and distribution of lattice defects and tendency towards martensite formation.[39)] In general, a lower SFE makes dislocation cross-slip more difficult, resulting in less dislocation mobility. This will favor more homogeneous dislocation distribution with less tendency towards the formation of dislocation cells. Also a larger amount of stacking faults and DIM formed during

cold working can be correlated to a lower SFE.[39] Deformation twinning is also dependent on SFE and grain size. Low SFE and large grain size favor deformation twinning. Recent work[40] has shown that deformation twin initiation requires a critical deformation (critical dislocation density). The SFE has an indirect effect by increasing dislocation density and strain hardening in low-SFE fcc metals and alloys.[40] Another aspect that must be remembered is that SFE of the ASSs increases with deformation temperature.[41] In summary, depending on the value of the SFE, two different microstructures may be observed in the cold worked ASSs: for a high SFE, a cellular dislocation distribution without DIM and, for a low SFE, a planar dislocation distribution containing DIM. It is worthy of note that deformation bands can be found in both.

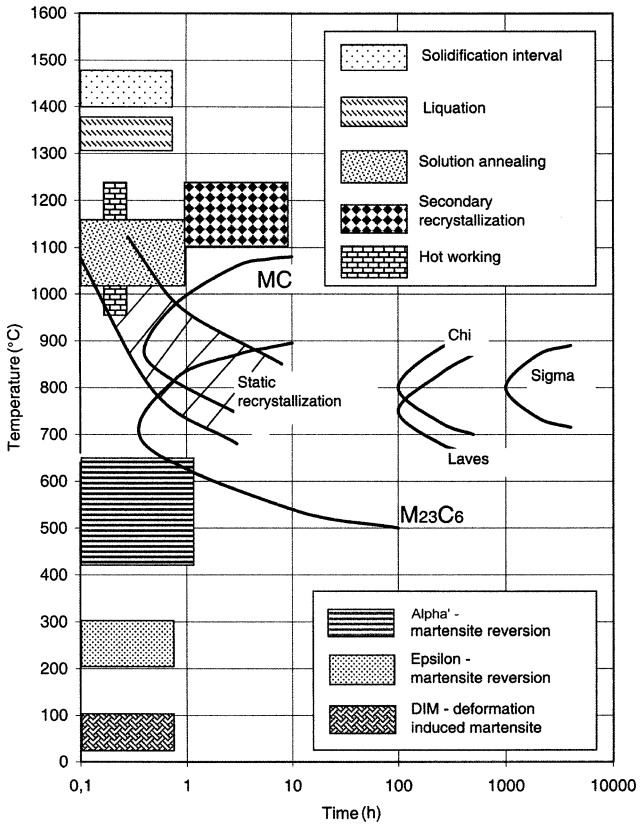

Fig. 1. Main thermal treatments and transformations that occur in austenitic stainless steels (ASSs) between room temperature and the liquid state.

In terms of recrystallization, the lower is the SFE, keeping all others variables constant, the larger will be the stored energy during deformation and the corresponding driving force for recrystallization. This subject will be discussed later on in greater detail.

ASSs are commonly considered to be materials having a low SFE. Actually the SFE of this class of steels are within quite a large range.[42–47] **Table 1** presents the SFEs of the more common ASSs, evaluated by means of the equation suggested by Schramm and Reed[44]:

$$\text{SFE (mJ/m}^2) = -53 + 6.2(\%\text{Ni}) + 0.7(\%\text{Cr}) + 3.2(\%\text{Mn}) + 9.3(\%\text{Mo}) \quad \ldots\ldots\ldots\ldots (1)$$

It may be observed from Table 1 that some steels, such as AISI 301 and 304, have very low SFE values. Other steels, such as AISI 316 and W. Nr. 1.4970, have higher values of SFE, close to those of copper.[48] An illustration of this is the cellular distribution of the dislocations found in the W. Nr. 1.4970, after cold working (see **Fig. 2**(b)). Several interesting features can observed in this figure. Microstructural analysis using optical microscopy, as shown in Fig. 2(a) for a high SFE ASS, does not allow differentiation between high and low SFE austenitic stainless steels after cold working. Furthermore, at the transmission electron microscopy scale deformation bands may be seen eventually (compare Figs. 2(b) and 2(c)). Monteiro and Kestenbach[49] using transmission electron microscopy observed that dislocation substructure is orientation sensitive, *i.e.*, individual grains develop different substructures, according to their specific orientation and the orientation of their neighbours.

As previously mentioned, two types of martensite may occur in the ASSs, namely: α'-(bcc, ferromagnetic) and ε-(hcp, paramagnetic). The typical lattice parameters are:

$$a_{\alpha'} = 0.2872\,\text{nm} \text{ and } a_{\varepsilon} = 0.2532\,\text{nm}; \quad c_{\varepsilon} = 0.4114\,\text{nm}$$

Assuming[50] $a_{\gamma} = 0.3585\,\text{nm}$, we may conclude that the $\gamma \rightarrow \alpha'$ transformation leads to volume increase of about

Table 1. Chemical composition (mass content in %) and stacking fault energy (SFE; mJ/m^2) of some ASSs.

Type	UNS Nº	Werkstoff Nr.	C	Mn	Si	Cr	Ni	Mo	Other	SFE (mJ/m^2)
301	S30100	1.4310	<0.15	<2.0	<1.0	16.0-18.0	6.0-8.0	---	---	<16
304	S30400	1.4301	<0.08	<2.0	<1.0	18.0-20.0	8.0-10.5	---	---	9.2-32.5
304L	S30403	1.4306	<0.03	<2.0	<1.0	18.0-20.0	8.0-12.0	---	---	9.2-41.8
316	S31600	1.4401	<0.08	<2.0	<1.0	16.0-18.0	10.0-14.0	2.0-3.0	---	34.6-80.7
316L	S31603	1.4404	<0.03	<2.0	<1.0	16.0-18.0	10.0-14.0	2.0-3.0	---	34.6-80.7
321	S32100	1.4541	<0.08	<2.0	<1.0	17.0-19.0	9.0-12.0	---	Ti>5 X%C	14.7-41.1
347	S34700	1.4550	<0.08	<2.0	<1.0	17.0-19.0	9.0-13.0	---	Nb>10 X%C	14.7-47.3
370(*)	S37000	1.4970	0.08-0.12	<2.0	0.3-0.55	14.5-15.5	14.5-15.5	1.0-1.4	Ti= 0.3-0.55	56.4-73.4
370	S37000	1.4970	0.08-0.12	1.6-2.0	0.25 0.45	14.5-15.5	15.0-16.0	1.05 1.4	Ti= 0.35-0.55	65.0-76.5

(*) German nuclear specification

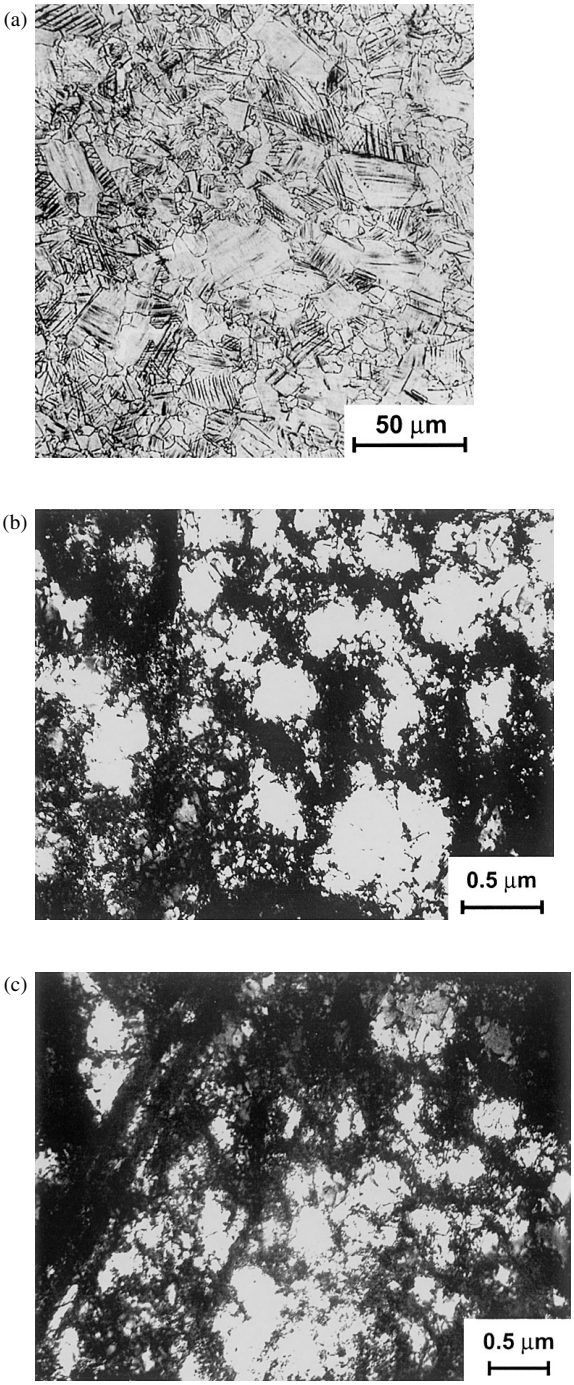

Fig. 2. Microstructure of cold-worked W. Nr. 1.4970 steel bar (15% reduction of area swaged at room temperature) (after A. F. Padilha, USP, Brazil): (a) Optical micrograph showing deformation lines within austenite grains; (b) transmission electron micrograph showing dislocation cells and (c) transmission electron micrograph showing deformation bands and dislocation cells.

2.6%, while the $\gamma \rightarrow \varepsilon$ cause a volume decrease of about 0.8%. The martensite phase formation is, therefore, related to the stress state given by the deformation process. In the ASSs the temperature below which austenite transforms spontaneously to martensite, M_s, is less than 0°C. M_s can be estimated with the help of the equation of Eichelmann and Hull[51]:

$$M_s\,(°C) = 1\,305 - [1\,667(\%C + \%N) + 28(\%Si) + 33(\%Mn) + 42(\%Cr) + 61(\%Ni)] \quad \ldots\ldots\ldots (2)$$

where the contents are in wt%.

Since M_s is low, martensite is not expected to form during the cooling of the ASS. This situation can be changed by $M_{23}C_6$ precipitation on the grain boundaries. This precipitation significantly decreases the carbon and chromium contents near those boundaries thus increasing M_s to temperatures higher than room temperature, leading to the possibility of α'-martensite formation.[52]

In contrast to M_s, M_d, temperature below which deformation stresses can initiate the martensitic transformation, is usually above room temperature. The temperature at which 50% of the α'-martensite is produced after 30% true deformation under tensile condition, can be evaluated with the help of the equation proposed by Angel[53]:

$$M_{d30/50}\,(°C) = 413 - [462(\%C + \%N) + 9.2(\%Si) + 8.1(\%Mn) + 13.7(\%Cr) + 9.5(\%Ni) + 18.5\,(\%Mo)] \quad \ldots\ldots\ldots (3)$$

Equations similar to Eqs. (2) and (3), evaluating the ε-martensite formation, were not found in the ASS literature.

The strain induced martensite transformation in the ASSs is influenced by the steel chemical composition and by the variables related to the cold working such as deformation, strain rate, stress state and deformation temperature. In general, the tendency towards martensite formation and martensite quantity increase with chromium equivalent, deformation level, deformation speed and decreases with nickel equivalent, SFE and deformation temperature. As to the stress state, Kaieda and Oguchi,[15] working with a 17%Cr–7%Ni–1%Al steel, showed that the M_s temperature decreases with an increase in pressure and that the formation of α' martensite induced by deformation was suppressed by increasing hydrostatic pressure.

Steels that present a higher M_d temperature, such as the AISI 301 and 304 are highly susceptible to the formation of DIM during deformation at room temperature,[1,7,10–12,14,16,18,20,22–24] whilst steels such as the AISI 316 and 321, with lower M_d temperatures, the formation of DIM is generally absent at room temperature working.[2,3,9,12,16,20] The W. Nr. 1.4970 steel has an extremely low M_d temperature and deformation induced martensite has never been detected.[4–6] An explanation for such a behaviour is that nickel has an accentuated effect in increasing the SFE,[44] and in suppressing the formation of DIM.[22] With respect to the increase in α'-martensite formation with the increase in strain rate[11,24] it is important to mention that the sample or test sample temperature can increase during deformation. Temperature gradients are therefore established between the center and surface of the sample, even in a tensile test, where strain rates are small. These thermal gradients due to mechanical working increase when strain rate is increased.[19] This effect is accentuated by the low thermal conductivities of the ASSs.

Some researches[9,12] show that for low deformation levels the amount of ε-martensite is predominant in relation to α'. When the quantity of α' grows continuously with the degree of deformation, the amount of ε-martensite goes through a maximum and lowers thereafter, suggesting the

following transformation sequence: $\gamma \rightarrow \varepsilon \rightarrow \alpha'$.

According to several authors,[1,7,8,12] DIM nucleates or starts at shear band intersections, that may be in the form of ε-martensite, deformation twins or dense bundles of stacking faults.

Finally, it must be pointed out that the ε-martensite as well as the α'-martensite present orientation relationships with the austenite. In the case of α' and γ, the relationships of Kurdjumov–Sachs as well as the relationships of Nishiyma–Wassermann are found.[12]

3. Martensite Reversion

Martensite reversion of the DIM in the ASS is less studied than its formation. A good judgment about the thermal stabilities of the ε- and α'-martensites, as well as the deformation bands introduced by cold working can be obtained from the work of Singh.[16] He detected that during annealing (with duration of 1 h) of a cold rolled AISI 304, α'-martensite remained stable up to 200°C, that α' was stable up to 400°C, whereas deformation bands stayed in non-recrystallized regions up to 800°C. Guy and co-authors[34] studied the reversion of α' induced by cooling and by deforming in two different steels (18%Cr–8%Ni and 18%Cr–12%Ni). In both cases, after 2 min at 600°C, practically all α'-martensite reverted to austenite. Martins and co-authors [35] studied α'-martensite reversion in the 304 and 304L steels and concluded that the reversion temperature was little sensitive to the type of steel, strain and the effect of precipitation treatments introduced prior to cold working. For the 12 studied conditions (2 steels×2 pre-treatments and 3 strain levels), the temperature (annealing for 1 h) for 50% α' ($T_{50\%RM}$) reversion was always within the 550±20°C range. Tavares and co-authors[36] studied α'-martensite reversion and observed that the $T_{50\%RM}$ depended only slightly on strain and heating rate. The temperatures, measured for 3 levels of strain and 3 heating rates, stayed between 549 and 573°C. Analysis of the above mentioned works[16,34–36] shows that reversion of the strain induced martensites in the ASS occurs in temperatures much lower than the recrystallization temperature, despite the complete reversion of α'-martensite, may reach temperatures of the order of 750°C. Several works[34–36] have shown evidence that reversion has components of an athermal shear mechanism and of an isothermal diffusional mechanism. An interesting phenomenon that occurs during annealing in cold worked ASSs is the increase in α'-martensite content when annealing is performed in the 300 to 400°C temperature range.[31,32,34,36] There are two alternative but compatible explanations for this phenomenon. Annealing at those temperatures leads to recovery mechanisms such as removal and/or rearrangement of point defects, dislocations and stacking fault defects, that, in turn, cause stress relieve around the martensite laths that may grow subsequently. The second mechanism takes into consideration carbide precipitation and consequently an increase in the M_s temperature and, therefore, more martensite is formed on cooling. This latter explanation is less likely possible since no carbide formation at such low temperatures has been detected in the ASSs.

4. Recovery and Recrystallization

Recrystallization of the ASSs occurs at temperatures about 100°C higher than the martensite reversion temperature. Recrystallization takes place only in the cold worked, γ-retained regions and not in the reversed γ.[34] Recrystallization begins on deformation bands and in the vicinity of grain boundaries.[35] There is no clear evidence that there is a correlation between the reversion of martensite and recrystallization.

Recrystallization of the ASSs in general and the recrystallization temperature in particular depend on several factors such as the steel type, the heat treatments that the steel might have been submitted before cold working, the quantity, mode, temperature and strain rate at cold working, as well as the heating rate and holding time at the annealing temperature. Due to the large number of variables and the complexity of the phenomena involved, it is not easy to specify a single recrystallization temperature of the ASS. For example, Lula[54] quotes 705°C (1 300 F) for recrystallization start, while other authors[55] report a range from 950 to 1 000°C and time intervals between 5 and 10 min. In general, all variables that increase the stored energy due to deformation such as a decrease in the stacking fault energy, increase in strain, increase in strain rate and decrease in deformation temperature, cause a decrease in the recrystallization temperature. For instance, Yang and Spruiell[56] comparing several steels, showed experimentally that the recrystallization start temperature in the ASS lowers with the decrease in the SFE. The same trend has been observed by Kestenbach[57] for a AISI 304 steel by changing the deformation temperature, who demonstrated experimentally that the cellular dislocation substructure is stable against recrystallization as compared to a planar dislocation distribution.

Particles that are present in the material after solution annealing and before cold working, such as carbides, nitrides, sulfides and oxides, are generally sufficiently large and widely spaced to induce recrystallization nucleation. This is usually called particle stimulated nucleation of recrystallization—PSN.[58]

Secondary carbides of the $M_{23}C_6$ and MC type precipitate in the same temperature range and times in which recrystallization occurs (see Fig. 1) and both phenomena present a strong interaction: cold working accelerates precipitation and precipitation delays recrystallization. In ASSs, the higher is the carbon content, the more difficult is recrystallization.[35] The transmission electron micrograph shown in **Fig. 3**, illustrates that for a non-stabilized steel that has a low SFE, such as AISI 304, recrystallization is the main softening process and that recovery plays a minor role. The temperature range in which precipitation of MC carbides occurs is higher (see Fig. 1), it coincides with the temperature range which recrystallization occurs, and its effect on recrystallization is more pronounced than for the $M_{23}C_6$ carbides. The overall effect of the precipitation of the MC secondary carbides during annealing of cold worked stabilized ASS is dubious. The effect mostly found and expected is that the precipitation of MC in the dislocation substructure, introduced by cold working, hinders dislocation rearrangement and delays recrystallization by grain boundary

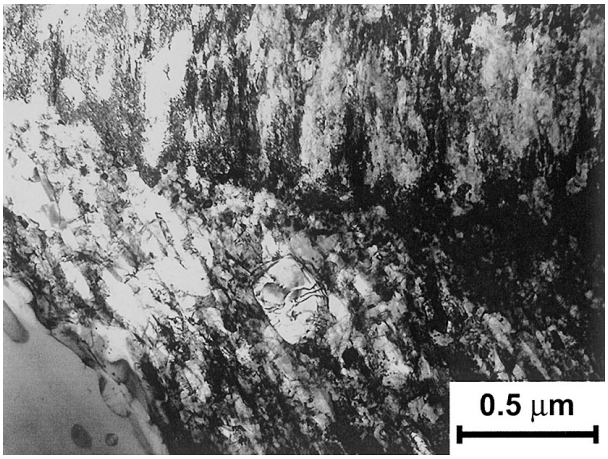

Fig. 3. Transmission electron micrograph of a 60% thickness reduction cold rolled AISI 304 plate, annealed for 1h at 700°C, showing the recrystallization start (after A. F. Padilha, USP, Brazil).

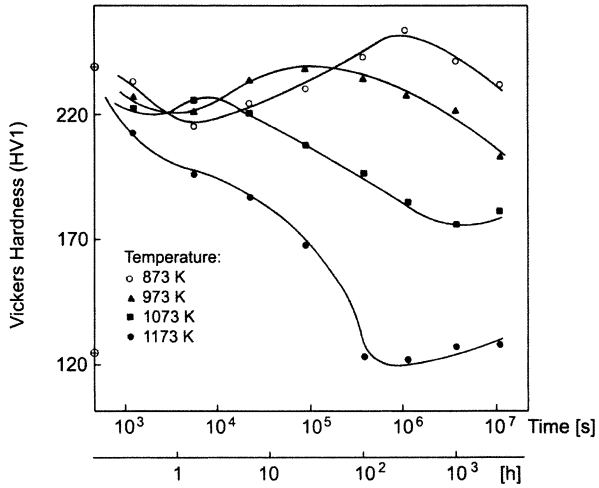

Fig. 4. Softening curves (hardness as a function of time) at 600, 700, 800 and 900°C for the W. Nr. 1.4970 steel cold swaged 15% reduction of area (after A. F. Padilha, USP, Brazil).

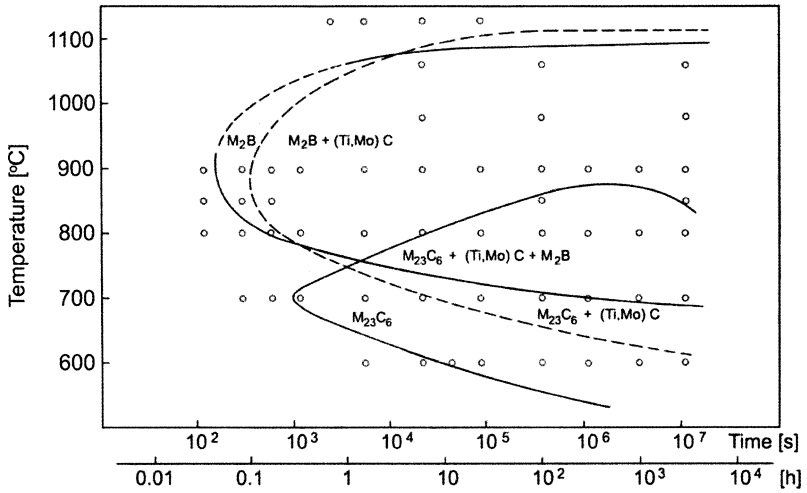

Fig. 5. TTP (Time Temperature Precipitation) diagram for the W. Nr. 1.4970 steel (after solution annealing 30 min at 1 130°C and cold swaged 15% reduction of area) (after A. F. Padilha, USP, Brazil).

pinning.[59,60] On the other hand, precipitation avoids the reduction of the recrystallization driving force through recovery and, therefore, can accelerate recrystallization.[61] The first effect predominates and the stabilized ASSs normally show a greater resistance to recrystallization as compared to the non-stabilized ones. The M/(C+N) ratio, where M is generally Ti or Nb, and the solution annealing temperature can be selected in such a way as to lead to a maximum delay in recrystallization.[60] **Figures 4** and **5** show the softening and the TTT diagrams for a Ti-stabilized steel, respectively.[62] Figure 4 shows the noteworthy recrystallization resistance of the steel. This recrystallization resistance is important for the performance of this steel as a cladding material for fast breeder nuclear reactors.[4–6] The transmission electron micrograph of **Fig. 6** illustrates the softening by recovery and the appearance of sub-grains at 800°C in this steel. Therefore, recovery is favored in the stabilized steels and/or in those having higher SFE. It must be pointed out that particles, in general, hinder grain boundary migration,[63] as shown in **Fig. 7**.

The interaction between recrystallization and precipita-

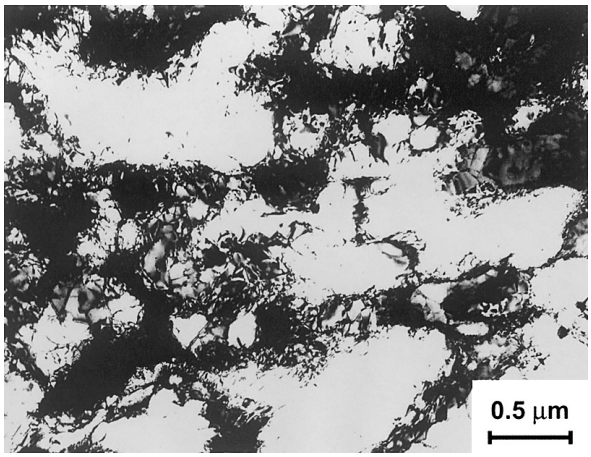

Fig. 6. Transmission electron micrograph showing subgrains in the W. Nr. 1.4970 steel after cold swaging 15% reduction of area and annealing for 3 000 h at 800°C (after A. F. Padilha, USP, Brazil). The corresponding hardness is given in Fig. 4.

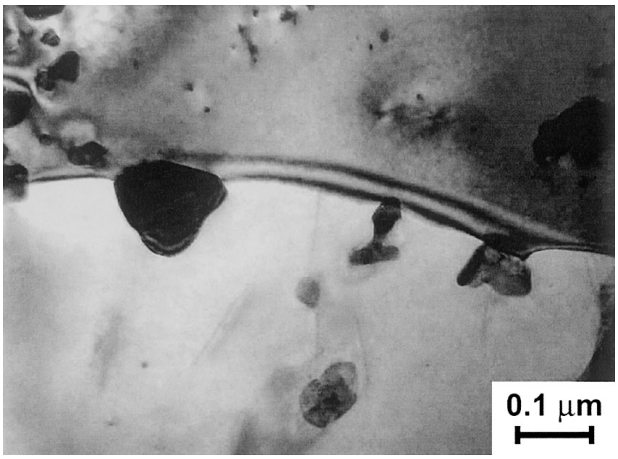

Fig. 7. Transmission electron micrograph showing the interaction between particles ($M_{23}C_6$) and migrating boundaries in cold rolled AISI 304 plate, annealed for 1 h at 700°C (after A. F. Padilha, USP, Brazil).

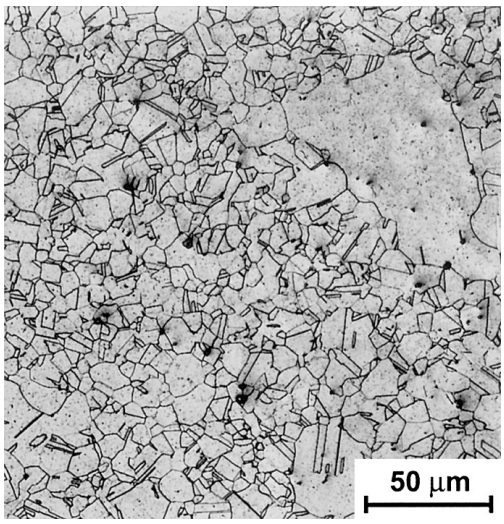

Fig. 8. Optical micrograph showing secondary recrystallization start in the W. Nr. 1.4970 steel after solution annealing for 30 min at 1 130°C (after A. F. Padilha, USP, Brazil).

tion of intermetallic phases is less frequent. For example, in the majority of the ASSs, the precipitation of sigma phase requires hundreds or even thousands of hours, and in some cases, years[30] to happen. On the other hand, there is experimental evidence[64,65] that shows that plastic deformation only accelerates the sigma phase precipitation when recrystallization occurs simultaneously with precipitation. As the σ- and χ-phases compete for chromium and molybdenum, an acceleration in the sigma phase precipitation may lead to a delay in the chi phase.[2,30] The precipitation of the chi and Laves phases generally comes before the formation of the sigma phase[25,26,30] and the probability of a simultaneous precipitation of these phases and recrystallization is even greater. These phases (chi and Laves) only occur in steels containing molybdenum and/or that they are stabilized and form in small quantities. For the formation of the chi-phase the steel must have at least 2% Mo and that the formation of Laves phases of type Fe_2M (M=Mo, Nb, Ti), needs Nb or Ti in excess in solid solution, i.e., non combined with carbon. While the Mo content in solid solution in these steels is needed for pitting corrosion resistance, the addition of Nb and/or Ti has to be optimized as a function of C content.

5. Grain Growth and Secondary Recrystallization

Primary recrystallization and grain growth take place by the migration of high angle grain boundaries. The driving force is of course different, for primary recrystallization it is the lattice defect energy, mainly dislocations, whilst the driving force for grain growth and for secondary recrystallization is the grain boundary energy.[66] Normal or continuous grain growth occurs gradually and results in an increase in the average grain size. The grain size distribution is monomodal and shows a time invariant behaviour. Abnormal or discontinuous grain growth (also known as secondary recrystallization) occurs when a few grains grow much faster than the average size of the normal grains. The initial grain size distribution can be monomodal but progresses through a bimodal stage and finally returns to a monomodal distribution constituted of the resulting abnormal grains. It is frequently observed that secondary recrystallization occurs when normal grain growth is restrained.[38]

Under 900°C, grain growth in the ASSs is very slow and this behavior can be attributed to several causes that are interconnected: sluggish diffusion in austenite, low mobility of high angle grain boundaries, particles and low driving force. Grain growth in the ASSs is significant only over 950°C in the non-stabilized and over 1 050°C in the stabilized ASSs.[38,67,68] In the stabilized steels, the risk of some abnormal grain growth or secondary recrystallization (see **Fig. 8**) is greater. **Fig. 9** shows that between 1 100 and 1 200°C the risk of secondary recrystallization, due to partial dissolution of the MC carbides, is very large.[38,67] Recent work[69] on high purity austenitic stainless steels showed that carbon, even in solid solution, hinders grain growth.

Randle and co-authors[37,70,71] showed that small amounts of cold working (2 to 7%), increase the tendency towards the appearance of coarse grains during annealing in the 900 to 970°C temperature range and attributed the fact of the occurrence of secondary recrystallization due to deformation (strain induced secondary recrystallization). On the other hand, the best interpretation is in terms of primary recrystallization by strain induced grain boundary migration rather than a grain growth phenomenon.[58] Despite both phenomena (primary and secondary recrystallization) involve grain boundary migration, their driving force and migration rate are quite different. Furthermore, during migration, their grain boundaries present opposite curvatures.

6. Resulting Textures

In this item the resulting textures of cold-rolling, primary recrystallization and secondary recrystallization will be discussed. Before discussing the cold rolling texture it is important to bear in mind the preceding texture, produced by the hot-rolling.

Although the hot-rolled strip generally reveals a weak orientation distribution, a considerable texture gradient occurs between the central layers and the surface layers.[72,73]

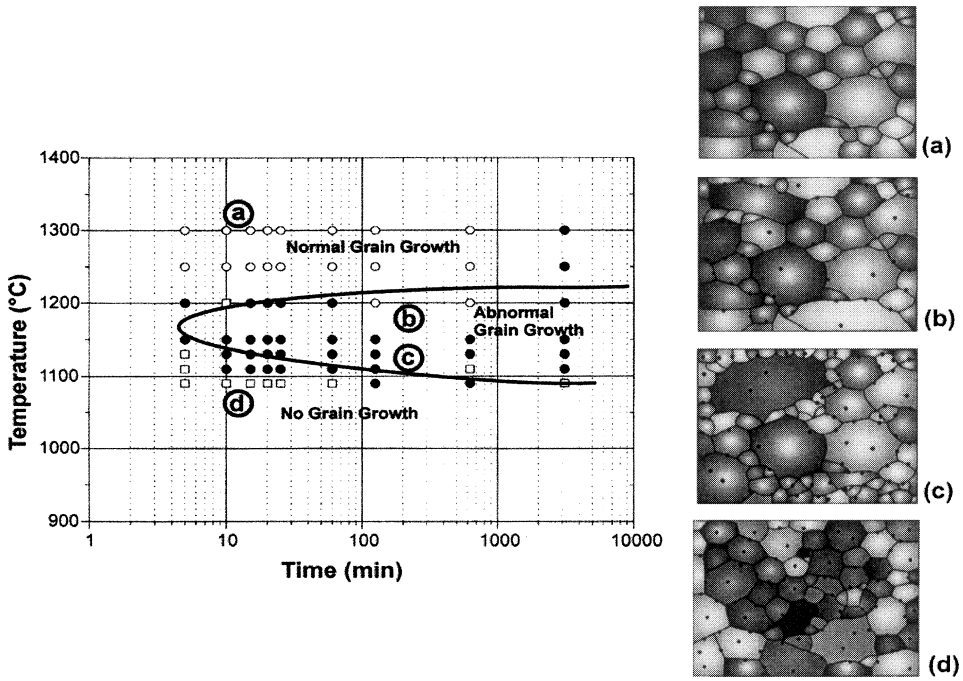

Fig. 9. Schematic representation of the different grain growth regions as a function of temperature and time for the W. Nr. 1.4970 steel (after J. C. Dutra,[38,67] FEI, Brazil).

The deformation texture consists mainly of {001}⟨110⟩, {111}⟨110⟩ and {112}⟨110⟩ in the severely sheared region, and mainly {110}⟨112⟩ in the mid-thickness.[72]

Goodman and Hu[74,75] found that the rolling texture of an 18.6%Cr–9.5%Ni (AISI 304) austenitic stainless steel changed gradually from the {110}⟨112⟩ brass-type to the {123}⟨412⟩ copper type as the rolling temperature (and the stacking fault energy) increased from 200 to 800°C. Similar results were found in an 18%Cr–9%Ni austenitic stainless steel after cold rolling.[76] The brass-type texture {110}⟨112⟩ also predominated in an AISI 316 L austenitic stainless steel after 40, 70 and 90% reduction by cold-rolling.[77] The cold rolling textures of 18% chromium steels containing 10, 12 and 14% nickel have been determined[78] and were again of the {110}⟨112⟩ type. The same rolling texture was found[79] in a 20%Cr–25%Ni niobium stabilized steel. In summary, it can be said that the cold-rolling textures of austenite in chromium–nickel steels may be, in many cases, adequately described by a strong {110}⟨112⟩ component and by several weaker components such as {110}⟨001⟩, {135}⟨211⟩ and {211}⟨011⟩.

When the deformed metal is annealed, recovery and/or recrystallization may occur, depending on the deformation strain, time and mainly annealing temperature. Generally, annealing at lower temperatures of materials with small deformation cause only recovery and small or nearly no texture modification. Annealing at higher temperatures leads to recrystallization. The texture of the recrystallized structure is usually different but related to the deformation texture. The results of recrystallization textures in austenitic stainless steels showed poorer consensus compared to cold-rolling textures. Nevertheless, in several investigations[76–79] the recrystallization texture was described as {113}⟨211⟩. Furthermore, many experimental results obtained with recrystallized non-ferrous fcc metals and alloys with low stacking fault energy were described in terms of the same orientation.[80] This orientation may be derived[78] from the {110}⟨112⟩ component of the rolling texture by a 40° ⟨111⟩ rotation. Dickson and Green [78] interpreted this as evidence of an oriented-growth mechanism.

After recrystallization, both continuous or normal grain growth, and abnormal or secondary recrystallization may occur. Normal grain growth is most commonly associated with a sharpening of the texture produced on primary recrystallization. During secondary recrystallization, few grains will grow consuming their smaller neighbours. The resulting texture, also in this case, is generally different from the deformation and recrystallization textures. In the same way that recrystallized grains grow in a deformed matrix and eventually replace it, recrystallized grains can themselves be replaced by a new set of grains growing larger at their expense. Examples where texture changes occurred during secondary recrystallization are known in several metals and alloys.[38] In a titanium stabilized austenitic stainless steel after secondary recrystallization[38] a strong {122}⟨012⟩ texture was found plus some {120}⟨210⟩ and {100}⟨012⟩ components. These textures did not coincide with any of the textures frequently found previously in fcc metals and alloys after secondary recrystallization.

7. Final Remarks

Annealing of cold worked austenitic steels is a complex phenomenon. In addition to the usual problems presented in the deformation and recrystallization of conventional steels deformation induced martensite and martensite reversion have also to be taken into account.

Greater understanding of the deformation and annealing of austenitic stainless steels has considerable practical importance with regard both to the formability of these steels and to the optimisation of their mechanical strength by means of thermomechanical treatments. Careful control of

the microstructure through thermomechanical treatments may lead to a five-fold increase in the yield strength of those steels. In terms of industrial production, it is necessary to establish relationships between microstructure and texture in metal working processes and the process variables, such as strain, strain rate and temperature of deformation and annealing conditions.

This review shows that in spite of the considerable amount of information available there are still critical issues to be investigated. More detailed investigations on the "nucleation" sites and "nucleation" mechanisms of ASSs primary and secondary recrystallization are desirable. Also a more in-depth investigation of the textures is still to be done, particularly with regard to the most favourable orientation relationships for boundary migration.

Another promising and yet hardly explored field in ASSs is mesotexture control, also known as grain boundary engineering, aiming at special boundary properties.[81,82]

Acknowledgements

The authors gratefully acknowledge the careful manuscript revision carried out by Professor Roger D. Doherty (Drexel University, USA). This work was supported financially by the Conselho Nacional de Desenvolvimento Cientifico e Tecnologico (CNPq) and FAPESP (contract 99/10796-8), Brazil.

REFERENCES

1) P. L. Mangonon, Jr. and G. Thomas: *Metall. Trans*., **1** (1970), 1587.
2) J. E. Spruiell, J. A. Scott, C. S. Ary and R. L. Hardin: *Metall. Trans.*, **4** (1973), 1533.
3) A. S. Grot and J. E. Spruiell: *Metall. Trans.*, **6A** (1975), 2023.
4) A. F. Padilha, G. Schanz and K. Anderko: *J. Nucl. Mater*., **105** (1982),77.
5) W. Kesternich and D. Meertens: *Acta Metall.*, **34** (1986), 1071.
6) M. Vasudevan, S. Venkadesan and P. V. Sivaprasad: *Mater. Sci. Technol*., **12** (1996), 338.
7) P. L. Mangonon, Jr. and G. Thomas: *Metall. Trans*., **1** (1970), 1577.
8) G. B. Olson and M. Cohen: *Metall. Trans.*, **6A** (1975), 791.
9) V. Seetharaman and R. Krishnan: *J. Mater. Sci.*, **16** (1981), 523.
10) S. S. Hecker, M. G. Stout, K. P. Staudhamer and J. L. Smith: *Metall. Trans*., **13A** (1982), 619.
11) L. E. Murr, K. P. Staudhamer and S. S. Hecker: *Metall. Trans*., **13A** (1982), 627.
12) M. W. Bowkett, S. R. Keown and D. R. Harries: *Met. Sci.*, **16** (1982), 499.
13) K. P. Staudhamer, L. E. Murr and S. S. Hecker: *Acta Metall*., **31** (1983), 267.
14) K. Takashima, Y. Higo and S. Numomura: *Philos. Mag. A*, **49** (1984), 231.
15) Y. Kaieda and A. Oguchi: *J. Mater. Sci.*, **20** (1985), 1847.
16) J. Singh: *J. Mater. Sci*., **20** (1985), 3157.
17) D. C. Cook: *Metall. Trans*., **18A** (1987), 201.
18) G. L. Huang, D. K. Matlock and G. Krauss: *Metall. Trans*., **20A** (1989), 1239.
19) A. Kumar and L. K. Singhal: *Metall. Trans*., **19A** (1988), 1021.
20) S. K. Varma, J. Kalyanam, L. E. Murr and V. Srinivas: *J. Mater. Sci. Lett.*, **13** (1994), 107.
21) S. G. S. Raman and K. A. Padmanabhan: *J. Mater. Sci. Lett.*, **13** (1994), 389.
22) A. Weiß, X. Fang, H.-J. Eckstein, C. Eckstein and W. Dahl: *Steel Res*., **66** (1995), 495.
23) J-Y.Choi and W. Jin: *Scr. Mater*., **36** (1997), 99.
24) W-S.Lee and C-F. Lin: *Scr. Mater*., **43** (2000), 777.
25) B. Weiss and R. Stickler: *Metall. Trans*., **3** (1972), 851.
26) J. K. L. Lai: *Mater. Sci. Eng.*, **58** (1983), 195.
27) R. Ayer, C. F. Klein and C. N. Marzinsky: *Metall. Trans*., **23A** (1992), 2455.
28) R. F. A. Jargelius-Pettersson: *Z. Metallkd*., **89** (1998), 177.
29) T. Sourmail: *Mater. Sci. Technol*., **17** (2001), 1.
30) A. F. Padilha and P. R. Rios: *ISIJ Int.*, **42** (2002), 325.
31) R. Montanari: *Mater. Lett*., **10** (1990), 57.
32) C. K. Mukhopadhyay, T. Jayakumar, K. V. Kasiviswanathan and B. Raj: *J. Mater. Sci*., **30** (1995), 4556.
33) H. Smith and D. R. F. West: *J. Materi. Sci*., **8** (1973), 1413.
34) K. B. Guy, E. P. Butler and D. R. F. West: *Met. Sci*., **17** (1983), 167.
35) L. F. M. Martins, R. L. Plaut and A. F. Padilha: *ISIJ Int.*, **38** (1998), 572.
36) S. S. M. Tavares, D. Fruchart and S. Miraglia: *J. Alloys Compounds*, **307** (2000), 311.
37) V. Randle and A. Brown: *Philos. Mag. A*, **59** (1989), 1075.
38) A. F. Padilha, J. C. Dutra and V. Randle: *Mater. Sci. Technol*., **15** (1999), 1009.
39) R. P. Reed: Austenitic Steels at Low Temperatures, ed. by R. P. Reed and T. Horiuchi, Plenum Press, New York, (1983), 41.
40) E. El-Danaf, S. R. Kalidindi and R. D. Doherty: *Metall. Mater. Trans*., **30A** (1999), 1223.
41) L. Rémy, A. Pineau and B. Thomas: *Mater. Sci. Eng*., **36** (1978), 47.
42) J. M. Silcock, R. W. Rookes and J. Barford: *J. Iron Steel Inst*., **204** (1966), 623.
43) R. Fawley, M. A. Quader and R. A. Dodd: *Trans. Metall. Soc. AIME*, **242** (1968), 771.
44) R. E. Schramm and R. P. Reed: *Metall. Trans*., **6A** (1975), 1345.
45) F-E. Teng, B. Yang and Y. Wang: *Metall. Trans*., **23A** (1992), 2859.
46) L. G. Martinez, K. Imakuma and A. F. Padilha: *Steel Res*., **63** (1992), 221.
47) W. Reick, M. Pohl and A. F. Padilha: *Steel Res*., **67** (1996), 253.
48) R. P. Reed and R. E. Schramm: *J. Appl. Phys*., **45** (1974), 4705.
49) S. N. Monteiro and H.-J. Kestenbach: *Metall. Trans*., **6A** (1975), 938.
50) D. J. Dyson and B. Holmes: *J. Iron Steel Inst*., **208** (1970), 469.
51) G. H. Eichelmann and F. C. Hull: *Trans. Am. Soc. Met*., **45** (1953), 77.
52) E. P. Butler and M. G. Burke: *Acta Metall.*, **34** (1986), 557.
53) T. Angel: *J. Iron Steel Inst*., **177** (1954), 165.
54) R. A. Lula: Stainless Steel, American Society for Metals, Ohio, (1989), 23.
55) W. Küpers: Nichtrostende Stähle, 2nd Ed., ed. by H. Ordenbach, Verlag Stahleisen mbH, Düsseldorf, (1989), 139.
56) S. W. Yang and J. E. Spruiell: *J. Mater. Sci*., **17** (1982), 677.
57) H.-J. Kestenbach: *Metall. Trans. A*, **8A** (1977), 213.
58) F. J. Humphreys and M. Hatherly: Recrystallization and Related Annealing Phenomena, 1st Ed. (reprinted with corrections), Pergamon/Elsevier Science, Oxford, (1996), 235.
59) E. J. Herrera, V. Ramaswamy and D. R. F. West: *J. Iron Steel Inst*., **211** (1973), 229.
60) M. Vasudevan, S. Venkadesan and P. V. Sivaprasad: *J. Nucl. Mater*., **231** (1996), 231.
61) T. M. Williams: Recovery and Recrystallisation in type 316 and FV548 austenitic stainless steels, 1st RISØ Int. Symp. on Metallurgy and Materials Science, ed. by N. Hansen, A. R. Jones and T. Leffers, RISØ, Roskilde, Denmark, (1980), 263.
62) A. F. Padilha: Dr.-Ing. thesis, Universität Karlsruhe (TH), Germany, (1981).
63) P. R. Rios: *Acta Metall*., **35** (1987), 2805.
64) A. J. Lena and W. E. Curry: *Trans. Am. Soc. Met*., **47** (1955), 193.
65) P. Duhaj, J. Ivan and E. Makovický: J. Iron Steel Inst., **206** (1968), 1245.
66) R. W. Cahn: Physical Metallurgy, 4th Ed., Vol. 3, ed. by R. W. Cahn and P. Haasen, North-Holland, Amsterdam, (1996), 2399.
67) F. Siciliano, Jr., J. C. Dutra, F. C. Pimenta, Jr. and A. F. Padilha: Proc. of the 1st Joint Int. Conf. on Recrystallization and Grain Growth, Vol. 1, Springer-Verlag, Aachen,Germany, (2001), 471.
68) J. K. Stanley and A. J. Perrotta: *Metallography*, **2** (1969), 349.
69) L. Gavard, F. Montheillet and J. Le Coze: *Scr. Mater*., **39** (1998), 1095.
70) V. Randle and A. Brown: *Philos. Mag. A*, **58** (1988), 717.
71) V. Randle: *Mater. Sci. Forum*, **113–115** (1993), 189.
72) T. Sakai, Y. Saito and K. Kato: *Trans. Iron Steel Inst. Jpn*., **27** (1987), 520.

73) D. Raabe: *J. Mater. Sci.*, **30** (1995), 47.
74) S. R. Goodman and H. Hu: *Trans. Metall. Soc. AIME*, **230** (1964), 1413.
75) S. R. Goodman and H. Hu: *Trans. Metall. Soc. AIME*, **233** (1965), 103.
76) V. I. Yushkov, R. A. Adamescu, Y. S. Machnev, T. M. Gapeka and P. V. Geld: *Mater. Sci. Eng.*, **64** (1984), 157.
77) C. Donadille, R. Valle, P. Dervin and R. Penelle: *Acta Metall.*, **37** (1989), 1547.
78) M. J. Dickson and D. Green: *Mater. Sci. Eng.*, **4** (1969), 304.
79) V. Randle: *Mater. Sci. Technol.*, **6** (1990), 1231.
80) G. Y. Chin: Metals Handbook, Vol. 8: Metallography, Structures and Phase Diagrams, 8th Ed., ed. by M. B. Bever, American Society for Metals, Metals Park, OH, (1973), 229.
81) V. Randle: *Acta Mater.*, **47** (1999), 4187.
82) M. Shimada, H. Kokava, Z. J. Wang, Y. S. Sato and I. Karibe: *Acta Mater.*, **50** (2002), 2331.